A Visual Analytics Framework for Spatiotemporal Trade Network Analysis

Hong Wang, Yafeng Lu, Shade T. Shutters, Michael Steptoe, Feng Wang, Steven Landis, Ross Maciejewski

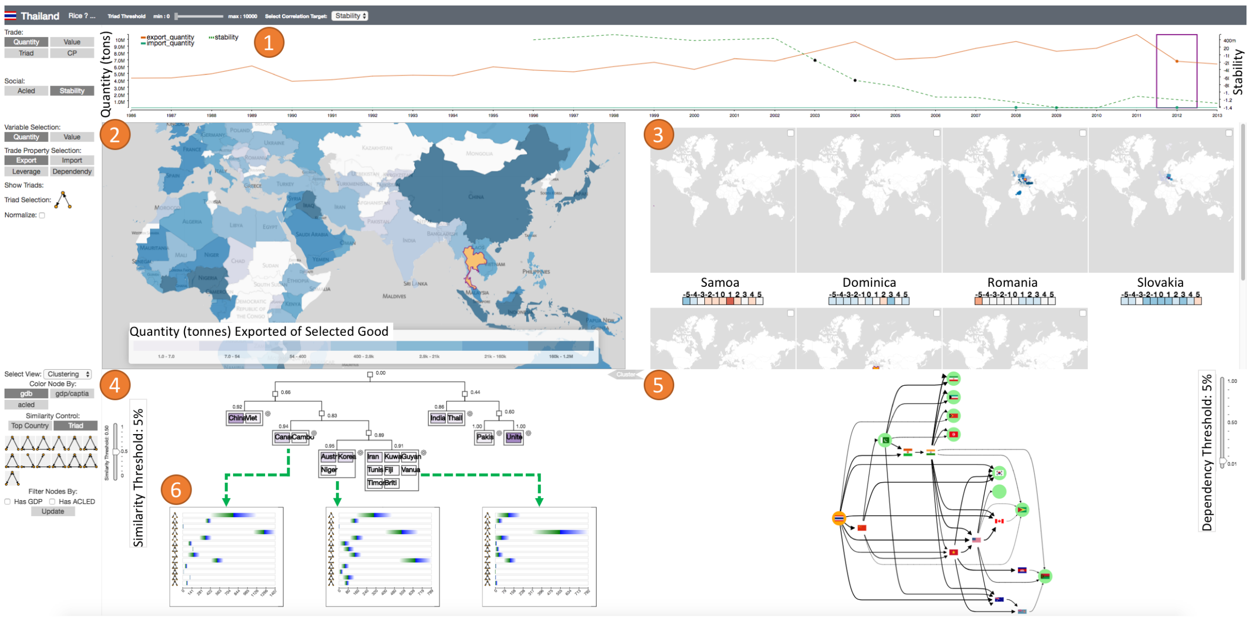

Fig. 1. A visual analytics framework for exploring global trade networks and their relationship to regional instability. The anomaly time series (1) on top displays the time series and anomalies of the trade attributes and stability measures for a selected country. The choropleth view (2) along with the small multiple maps (3) display the first order trade relationships centering on selected countries. The colored bars below each small multiple map show the temporal correlation of the selected trade measure to the stability measure. The clustering view (4) displays the hierarchical clustering for the countries, based on either the triadic similarity or top partner similarity. The groups can also be configured to show the average triad distributions (as (6)) and other measures. The trade diffusion graph (5) displays the propagation effect of anomalies. Connections between the nodes indicate the import dependency from the target node to the source node is larger than a threshold, which can be adjusted using the slider on the right.

Abstract—Economic globalization is increasing connectedness among regions of the world, creating complex interdependencies within various supply chains. Recent studies have indicated that changes and disruptions within such networks can serve as indicators for increased risks of violence and armed conflicts. This is especially true of countries that may not be able to compete for scarce commodities during supply shocks. Thus, network-induced vulnerability to supply disruption is typically exported from wealthier populations to disadvantaged populations. As such, researchers and stakeholders concerned with supply chains, political science, environmental studies, etc. need tools to explore the complex dynamics within global trade networks and how the structure of these networks relates to regional instability. However, the multivariate, spatiotemporal nature of the network structure creates a bottleneck in the extraction and analysis of correlations and anomalies for exploratory data analysis and hypothesis generation. Working closely with experts in political science and sustainability, we have developed a highly coordinated, multi-view framework that utilizes anomaly detection, network analytics, and spatiotemporal visualization methods for exploring the relationship between global trade networks and regional instability. Requirements for analysis and initial research questions to be investigated are elicited from domain experts, and a variety of visual encoding techniques for rapid assessment of analysis and correlations between trade goods, network patterns, and time series signatures are explored. We demonstrate the application of our framework through case studies focusing on armed conflicts in Africa, regional instability measures, and their relationship to international global trade.

Index Terms—Global trade network, anomaly detection, visual analytics

- *H. Wang, Y. Lu, S.T. Shutters, M. Steptoe, and R. Maciejewski are with Arizona State University. Email: {hxwang, lyafeng, Shade.Shutters, msteptoe, rmacieje}@asu.edu.*
- *S. Landis is with University of Nevada. Email: steven.landis@unlv.edu*
- *F. Wang is with GE Global Research. Email: Feng.Wang1@ge.com*

Manuscript received xx xxx. 201x; accepted xx xxx. 201x. Date of Publication xx xxx. 201x; date of current version xx xxx. 201x. For information on obtaining reprints of this article, please send e-mail to: reprints@ieee.org. Digital Object Identifier: xx.xxxx/TVCG.201x.xxxxxxx

1 Introduction

Economic globalization connects regions of the world and creates complex interdependencies among countries. Through trade connectivity, the risks associated with climate-induced changes in agricultural production (e.g. floods and droughts) are exported from areas with localized disruption to distant parts of the globe [49]. For instance, the monsoons of Southeast Asia may seem to have little to do with food supplies in distant parts of the world. However, when one considers that countries as distant as St. Kitts in the Caribbean and Congo in Africa both rely on Thailand for over 95% of their imported rice, it becomes clear that a significant disruption in Thailand's agricultural production could have a dire impact on food security thousands of miles away. Without an appreciation of the effects of global networks, attempts to mitigate social and economic disruption may lead to investment, for instance, in countries expecting drought and not in countries that will face food shortages due to that drought. However, food and water vulnerability are typically forecasted for demarcated and isolated units – regions, countries, subnational units, cities – while ignoring the impact of connections to other units (e.g. [54]). Little has been done on how a trade network topology contributes to the delocalized vulnerability of food and water delivery systems, insights that are crucial to planning for sustainable and resilient access to food and water. Furthermore, it is important to understand how trade network topology and network-induced food risks contribute to distant political instability and social unrest [36, 53, 76]. While the network of global trade has been well-studied, those studies are largely limited to characterizing the magnitude of exports between countries [18,19,28,40], the quantities of virtual water transmitted through those exports [17, 44, 72], or identifying the largest and most connected nodes in the network [5, 27, 29, 69].

Currently, what is needed are tools and methodologies that enable users to explore complex aspects of local trade structures and their relationships to local vulnerabilities. Recently, the visual analytics community has begun developing tools for analyzing complex global events. For example, geo-social relationships to the global trade network have been visually explored [48], and the relationship between climate change and human conflict has been analyzed through linked geographical visualizations and statistical analytic views [46,47]. Other analyses have called attention to how human migration might affect international trade [23] and how international trade may contribute to national air pollution [41]. Current methods have focused on geographic flow relationships [7, 32], movement of individuals and ships [67, 68], and spatiotemporal event detection [12, 13]. However, current methods have been limited to single temporal snapshots of flow and anomaly detection on space-time, ignoring networked effects. Understanding how trade relationships impact local vulnerabilities over time requires new methods that can provide an integrated analysis of local disruptions.

In the context of geographic network and flow analysis, common visualization methods quickly succumb to issues of overplotting. Geographic relationships need to be maintained to enable quickly filtering and exploring country relationships within a familiar spatial representation. However, as the number of attributes per country becomes large, and as the number of flows under analysis increase, methods for identifying data relationships and anomalies becomes critical. As such, this problem lends itself to a visual analytics approach where an analyst is needed to contextualize the geopolitical relationships of trade while being able to quickly cluster, filter and explore the data space. Our contributions include a visual analytics framework for combining multiple existing visualization techniques to help complement the user in processing large geographical data and their topological network relationships. This work introduces the concept of exploring triadic closures [71] over time, and by linking various triadic analysis features (a detailed explanation of triad analysis is provided in Section 3.3) with anomaly detection, we enable advanced filtering to help analysts identify unexpected patterns over feature space, time and network topology. Furthermore, the application of lead/lag time series analysis coupled with small multiples and clustering provides users with a novel mechanism to compare similarities of attributes between countries which possibly responded to the same known external disruptions in the network. We also explore the use of a diffusion graph to visualize the trade influence over countries, coupled with cluster analysis. Finally, the integration of correlation analysis with anomaly detection enables a novel visual analysis of the impact of trade-related anomalies on social instability, creating new mechanisms for hypothesis generation.

In order to identify challenges and needs in this area, we engaged in an iterative design procedure with collaborators in Sustainability and Political Science. From our discussion, a basic structure of analysis was defined (detailed in Section 4) and framework components identified. The basis of analysis is supported by an interactive map to visualize both the volume and proportion of trade events for imports, exports, and triadic structures. Temporal correlation analysis and anomaly detection are integrated to guide the user to structures of interest within the data, and small multiples are used to allow comparisons between regions with similar anomalies. Other views include a trade diffusion graph which explores the propagation effect of trade anomalies and a hierarchical clustering view which groups countries based on their triad profile similarities or trade partner similarities. Our key contributions include:

- An identification of design requirements for the exploratory visual analysis of global trade and regional unrest as elicited from our partners in political science and sustainability, as well as recent literature on global trade analysis;
- A novel triad analysis for exploring network dependencies to identify possible relationships between trade network structures and other measures of interest (e.g., social unrest), and;
- An integration of space, time, and network analysis methods to support the linked analysis of trade network data and conflict events through anomaly detection and correlation analysis across imports, exports and triadic structures.

Overall, our work advances previous visual analytics methods in this area by providing a novel correlation and triad anomaly detection proceudre to reduce the analysis search space. We utilize a suite of well-known visuals and provide several customized views to support advanced data exploration and hypothesis generation.

2 Related Work

The goal of our framework is to support the visual analysis of international global trade data and its relationship to regional instability. This work builds on previous work in geographic network analysis and visualization, anomaly detection and correlation analysis.

2.1 Geographical Network Visualization

In the global trade dataset, countries serve as nodes, and directed edges represent the quantity (or value) of goods imported or exported between countries. Such a structure directly corresponds to traditional origin-destination matrix data structures, and numerous methods for visualizing geographic flows have been developed. Early tools include Flow Mapper [75] which was used to create movement maps showing volume-scaled bands. Work by Dodge and Kitchin visualized the Internet infrastructures using flow maps [20]. Work by Cox et al. [15] and Munzner et al. [58] extended the concept of flow maps into 3D space. Guo [31] used flow maps to explore multivariate data, and Boyandin et al. [8] visualized migration flows over time using animation.

Central to these visualizations was the development of algorithms for placing flow lines in the 2D geographic space to maximize planarity while being aesthetically pleasing. Work by Phan et al. [60] developed an algorithm for defining the layout of flow maps utilizing hierarchical structures within the data. Cui et al. [16] implemented a control mesh method for flow line layouts, and Buchin, Speckmann, and Verbeek [9] introduced the spiral flow map which utilized angle-restricted Steiner arborescences to bundle lines smoothly and avoid self-intersection when creating flow maps. Other design strategies to alleviate clutter on flow maps include edge bundling [10, 35, 59] and information aggregation methods [2, 3, 62]. Alternatively, filtering selected flows [75] and filtering to a single limited set of origins or destinations [60] are also used to solve the occlusion problem. However, few works (e.g. [7]), have focused on spatiotemporal geographic network structures. Given the density of edges within our data and the need to explore trade patterns of countries, our design focuses on a choropleth map approach such that a choropleth map of country A's trade patterns can be directly compared (or even a difference taken) to country B.

Along with visual methods for geographic flow layouts, the topology of spatial interactions have also been studied with an emphasis on each connection's origin and destination. Wood et al. introduced OD map [79] which integrates node-link graphs and an OD matrix by dividing geographic space into a regular coarse grid and using each cell to represent the origin and the destination. The OD map was later extended by Yang et al. [80] into a MapTrix visualization which is a side-by-side view of a flow map and OD matrix for many-to-many geographical flow analysis. However, MapTrix was specifically designed as a static visualization to explore densely connected many-to-many flows. Boyandin et al. proposed Flowstrates [7], which is a temporal OD data visualization. It connects a temporal heatmap with two geographical maps presenting the geographical locations of origin and destination and shows how flow changes over time. Each row corresponds to a single flow as it uses columns for the temporal scale.

Our analysts are less interested in a global trade structure, but more interested in local trade structures and comparison between subgraphs (local structures of countries). Furthermore, our domain experts indicated that the topology of connections between importers and exporters is more interesting than their geography, as well as changes in the topology and local patterns over time. For visualization, this complicates the design space as overlapping graphs on geography or comparing graphs between small multiples would be difficult. As such, we focused on summary measures of network structures (i.e., triads); however, future work should consider visual summaries that can highlight and summarize structural changes in the network over time.

2.2 Event Detection Visual Analytics

While our domain experts indicated that network topology and connections were critical, the other requirement was to identify changes within the network over time and link these topological changes to measures of local instability. Event detection and temporal data analysis is a well-studied topic in visual analytics [14], and a variety of methods have been developed. LeadLine [21] supports event detection and annotation for topic exploration in streaming text discourse. Malik et al. [52] proposed a spatio-temporal visual analytics system which uses correlative analysis to detect trends and patterns. Work by Chae et al. [13] utilizes a seasonal-trend-decomposition method to determine anomalous changes in topics in social media. Scatterblogs [74] utilizes control chart methods to find unusual peaks and outliers within social media topic time series. Gotz et al. developed DecisionFlow [30] which supports a range of sequence analysis tasks of high-dimensional temporal event sequence data using interactive coordinated views and statistical models. Lu et al. [46] used intervention models and visualization cues to assist analysts in detecting time series anomalies in media framing. Similar to these works, we also employ time series anomaly detection method to find potential points of interest in the trade event time series. However, international trade events are complex and multivariate and instead of presenting all possible drivers or effects of the anomaly, our framework uses correlation analysis to further analyze the relationship between the trade data and instability measures. We use a network structure analysis technique, triad analysis (Section 3.3), to support the correlative analysis, and link our data to secondary data sets that document instability. This network exploration differs from previous visual analytics work in that instead of looking at event counts over time, we are attempting to summarize network structure properties through triads and correlate these to changes of network variables.

3 Global Trade Analytics

Our aim is to support domain experts from political science and sustainability to explore relationships between international trade structures and regional stability measures (e.g., national economic development measures and regional conflicts). In our initial discussions with our stakeholders, our goal was to elicit their analytic tasks and requirements. We then formatted the requirements of the framework based on the rationale of the targeted analysis from experts as well as relevant literature in trade analysis [55, 70, 82].

3.1 Data Description

To study the relationship between international trade events, country stability, and human conflicts, our domain experts have collected and provided international trade data [1], Armed Conflict Location Event Data (ACLED) [63], and economic data.

Trade Data: The trade data comes from the United Nations Food and Agriculture Organization (FAO) [1], and contains worldwide bilateral trade information of agriculture products. Each record in the data represents the total volume of trade occurred between two countries within one calendar year, and each record has 6 attributes: year, exporting country, importing country, the product of trade, trade quantity in tons, and trade value in dollars. The global trade data is available from FAOStat [1] and has been aggregated yearly from 1986 to 2013. The original data contains 600 types of agriculture products, many of them are very similar, such as “Meat, pig” and “Meat, pork”. Our collaborators have grouped the trade products into 20 categories creating a two-level hierarchy. As such, the trade network data consists of approximately 8.8 million trade records over 245 countries and territories with 20 product categories made up of approximately 600 individual goods. This means that there are nearly 150,000 possible networks when considering countries, product categories and individual goods (even more for group combination selections).

Stability Data: We make use of the Worldwide Governance Indicators (WGI) dataset [42], which reports aggregate governance indicators for over 200 countries and territories from 1996 to 2015. The original data contains a six-dimensional governance index. Our collaborators focus on the “Political Stability and Absence of Violence/Terrorism” governance index which ranges approximately from -2.5(weak) to 2.5(strong); high governance index indicates high stability.

Economic Data: We have also collected the GDP data from the world bank. It contains GDP and GDP per capita data for 265 political entities from 1960 to 2015, some of the political entities are continents. We only use data that overlaps with countries in the FAO data.

3.2 Design Requirements

When beginning the framework development, our analysts from sustainability and political science identified the primary question that they wanted to ask of their data: “Are there topological network structures associated with trade that serve as potential indicators of future instability?” Based on our discussions, it is clear that this topic has received much attention from their communities; however, our domain experts had identified current limitations in studying global trade networks. Specifically, many studies that do attempt to study the topology of food trade networks suffer from three typical simplifications that, while making analysis more tractable, may significantly distort conclusions:

- Aggregating commodities into a single network of “trade” (e.g. [19, 65]) - this ignores the flow of individual commodities and the relative importance of each.
- Ignoring the intensity, or weight, of trade (e.g. [28, 65]) - these studies consider only whether trade exists between country A and B, but disregard the magnitude of that trade. This ignores power differentials between countries, economies of scale, and concentrations of resources in specific regions of the network.
- Ignoring the directionality of the trade (e.g. [24, 64, 65, 72]) - perhaps the most egregious simplification is that an importer and exporter are treated equally and the direction of the flow of goods, transfer of risks, and shifts in power are ignored.

As such, our experts wanted a system that could allow for both aggregated and disaggregated food networks. We also discussed the fact that the combination of goods and years results in over 150,000 networks and this number is growing over time. What they required was a tool that could highlight time periods where large changes in the network structure were occurring and when these changes were correlated with changes in the various stability or economic measures that they had collected (e.g., ACLED events, stability indicators, and GDP). As such, our design rationale follows the visual analytics mantra proposed by Keim et al. [43], “Analyze first, show the important, zoom, filter and analyze further, details on demand,” and we have formulated several design requirements for our proposed framework.

R1 The framework needs to provide an overview for the expert to start their analysis given the sheer number of possible networks, each of them can be centered on many possible countries. This

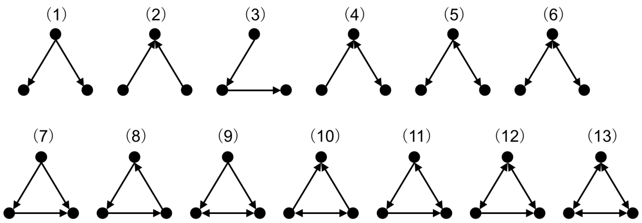

Fig. 2. The 13 possible triad configurations are labeled with numbers in braces. In the first row, triad 1 to 6 are open form triads, while in the second row, triad 7 to 13 are closed form triads.

overview needs to visualize patterns detected from the networks and the possible relationships between the network and local instability to help the expert select the data needed to be explored.

R2 Explorations of a trade network should be supported for the investigation of different trade measures, e.g., imports, exports, and reliance, and the structure of country's local network topologies.

R3 The framework needs the capability to show the possible influence between countries on their trade network. This is important to analyze the impact of food shortage on the network, and how such impact could further link to a country's stability disruption.

R4 Statistical analysis, such as correlation analysis and anomaly detection, should be integrated to assist the expert in generating and verifying hypotheses.

R5 The framework needs to retrieve similar countries based on the selected anomaly, and allow the expert to compare the trade networks involved with these countries. Supporting this is critical for the expert to generalize their findings.

In this problem domain, we have analysts that need views of space, time, and network connections of entities. Spatial views need to allow quick reference to regional variations in form analysts are familiar with (e.g., country level choropleth maps), while the temporal components need to be designed to help explore lags and leads. Critical to this is identifying regions that have similar temporal trends to a country of interest. If known disruptions have occurred in country A, analysts want to explore if other countries are experiencing similar trends as this may indicate upcoming disruptions (e.g., social unrest or violence). This suggests the needs for multiple views designed to link spatial regions for selection, highlight common attributes amongst regions for clustering, and identify unexplored regions that exhibit similar temporal and network dynamics that may have been leading indicators of unrest in known problem areas.

3.3 Triadic Analysis

Our domain experts also had specific requirements for analyzing local network attributes. Specifically, they wanted to explore triadic structures of the global and local trade patterns. Characteristics of trade networks, as with other types of networks such as social networks, biological networks, and economic networks, can be revealed by analyzing local structures. For example, if country A imports a specific product from both country B and country C, a competitive relationship may arise between B and C. The nature of this relationship also depends on the product flows between B and C and the types of products flowing between all three countries. To analyze these effects of local structure in a directed network, researchers typically analyze the network's triads, or subsets of three connected nodes. In contrast to dyads, triads are the smallest structures within a network that exhibit truly social characteristics [25, 33, 77]. The use of triads has long been a standard methodology in the study of networks [25], particularly with regard to properties such as structural balance [11] and transitivity [34]. While larger subgraphs can also be studied (e.g. tetrads), triads are a logical starting point for directed networks because the relatively small number of possible configurations are manageable for exploratory analysis [55].

A triad is a three-node directed subgraph, of which there are 13 configurations (grouped triads) (Fig. 2). When a network represents international trade, a triad can be viewed as a group of three countries and their associated trade interactions. The reasons we use triads, instead of dyads (two-node relationship) are: 1) Dyads result in fewer trade patterns when compared to triads, and therefore using triads may provide a finer characterization of the network's local pattern; 2) Bonds coincide more with triads than dyads, and; 3) Triads can be considered as more stable than dyads because a triad describes a relationship among three countries which is less easy to change [81].

Triadic analysis has revealed previously unknown structural attributes of networks that appear to be fundamental to a wide variety of natural, social, and man-made systems [39, 55, 56, 61, 78]. For instance, one of our collaborator's previous studies shows that countries at different stages of economic development have different triadic profiles [70]. As such, our collaborators were interested in analyzing how these triadic patterns within trade networks affect a country's vulnerability. Collapsing a network into a triad profile enables users to compare across a variety of network sizes and types and to identify triads that occur more or less frequently than expected [55, 82]. In addition, each triad has particular properties (e.g., transitivity) associated with conflict and reciprocity in social interactions [34]. These properties can help explain local differences and global patterns in networks which map human social interactions [22, 61, 73].

Several studies have used triadic analysis to study relationships between countries [4, 40, 45, 57]. However, while researchers generally agree that triadic analysis is a crucial methodological component of analyzing international relationships, there is no general agreement on what triads tell us about those relationships. To better understand the value that triadic analysis offers for the study of the global network, and to generate meaningful hypotheses, there is a need for a generalized platform to explore the triadic structure of international networks, such as trade networks, and global outcomes, such as country-level stability. Thus, our framework integrates triads to support trade network analysis. Grouped by triad selection, our framework supports anomaly detection, correlation analysis, clustering and similarity comparisons.

3.4 Dependency and Leverage

Besides measuring the absolute value of trade quantity/values from one country to the other, our collaborators also required a means of exploring dependency and leverage between countries. This measure is calculated based on the percentage of the quantity/values of the trade relationship over the total import quantity/values of the importing countries. More precisely, let c_i denote the exporting country and c_j the importing country, and the amount of exports from c_i to c_j denoted as $Q_{c_i \to c_j}$, then we can calculate the percentage of export from c_i to c_j over all imports to c_j as:

$$I_{c_i \to c_j} = \frac{Q_{c_i \to c_j}}{\sum_k Q_{c_k \to c_j}}$$

A large $I_{c_i \to c_j}$ indicates that c_j is dependent on c_i, conversely, it also means c_i holds a leverage on c_j and in this case c_j is susceptible to having a short supply of the trade products when c_i stops export to c_j.

4 Visual Analytics Framework

Based upon the design requirements and analytical needs discussed in Sec. 3.2, we developed a visual analytics framework to facilitate the exploration of relationships between international trade data and measures of a countrys stability. Our framework (Fig. 1, Fig. 3) consists of 5 major components designed to support the design requirements (R1-R5). 1) The country-product matrix (Fig. 3) which highlights the significant correlations and anomalies for each country/item pair (**R1**, **R4**). 2) The time series view (Fig. 1(1)) that displays the trend and anomalies of trades and stability measures for the selected country (**R4**). 3) The choropleth map view (Fig. 1(2)) that displays the trade profile of a selected country (**R2**), along with a small multiple of choropleth maps (Fig. 1(3)) used to compare the trade profiles of related countries to the selected one (**R5**). 4) The clustering view (Fig. 1(4)) and scatter plot view (Fig. 7(3)) are used to explore the similarities and differences of each country's trade profiles and compare trade profiles to stability measures (**R5**). 5) The trade diffusion graph (Fig.1(5)) displays the

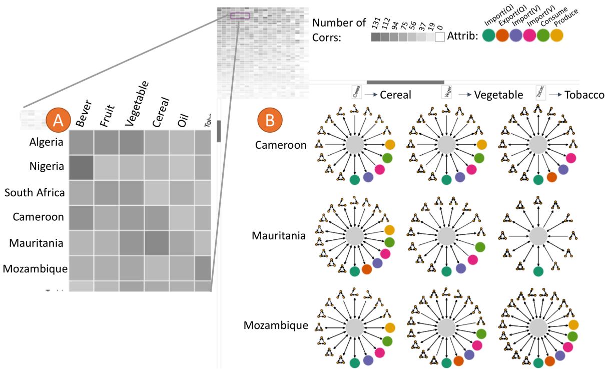

Fig. 3. The Country-Product Matrix view has an abstract view (A) and a detail view (B) to show the correlations between countries' trade and stability measures. This figure shows Cameroon and Mauritania have many correlations between cereal trade measures and ACLED events.

trade flow of the selected food products from the selected country to the countries whose disruption in trade are affected or affecting the selected country (**R3**).

A sample analytic flow can be described as: 1) The analyst uses the matrix view to find the countries and food products whose trade profile exhibits a temporal pattern that is strongly correlated with the stability measures. 2) Given the selection, the time series view will display the trend of trades along with the trend of stability measures and mark the anomalies. The analyst can select a time range by brushing on the time series or clicking on an anomaly. 3) After a time range is selected, the analyst uses the choropleth map to examine the trade relationships between the selected country and other countries and uses the small multiple of maps to compare the country of interest to the trade profiles of countries that exhibits the similar anomalous pattern. 4) The analyst then uses the network diagram to explore and hypothesize on the propagating effect of trade disruptions from/to the selected countries. 5) Finally, using the clustering view and scatter plot view, the analyst explores how the selected country's trade profile compares among other countries and examines whether countries with similar trade profiles also share similar social stability measures.

This sample analytic flow highlights the basic structure of our framework. Here, each view and analysis process was chosen to support specific tasks of the analysis, where we need to support the coupled interactions of space, time, and network analyses. By supporting multiple linked views, we can facilitate the switch between these three concepts. Furthermore, by providing methods of clustering and filtering across measures in space, time and networks, our proposed framework enables the integration of these concepts for advanced analysis.

4.1 Correlation-based Country-Product Matrix

Due to the large number of possible networks, the system provides a country-product matrix view to browse for interesting networks. In this view (Fig. 3), countries and products are presented as rows and columns. Each cell in this matrix visualizes the correlations between trade measures and stability measures given a country and a product.

This matrix view consists an abstract view (Fig. 3A) and a detail view (Fig. 3B). The abstract view provides an overview for the temporal correlations between each country's trade profiles and its stability measures with respect to 20 food categories. The color of the cell represents the total number of correlations, the darker, the higher. To help identify countries/product groups with large numbers of correlations, the matrix, by default, is ordered using a 2D sort method [50] to shift darker cells to the top left corner. The analyst can browse the matrix using the country slider on the left and the product slider on the top. A snapshot of the whole matrix is displayed on the top left corner to help keep track of the current location within the matrix, which is highlighted using a purple border in the snapshot. Customized reordering is also supported. The analyst can click on the "row" or "col" button on the top-right corner to order rows or columns based on the sum of correlations for each row or column. S/he can also click on a particular row (country) to sort columns (products) based on the number of correlations associated to this country and sort the countries based on their similarities of the indicated correlation patterns to this country. In addition, S/he can click on on a particular column (product) to sort countries based on the number of correlations in this product.

Once interesting cells are found, the user can brush over the cells to zoom in and switch to the detail view, which displays individual correlations. For any pair of trade metric and stability, we calculated the pairwise Pearson's correlation coefficients for leads/lags between -5 and 5. In the detail view, each cell is expanded with more information. The trade attributes with correlations are displayed in a circular layout surrounding the stability measure (colored in gray). The arrows connecting them indicate the directions of the correlations: if the correlation occurs when the trade attribute lags the stability measure, the arrow points from the trade attribute to the stability measure. Conversely, if the stability lags the trade attribute, the arrow points to the trade attribute. Double-direction arrows indicate lags in both directions.

These correlations only provide a hint of possible connections between the trade and stability for the countries. Some identified correlations may be spurious. However, these correlations serve as a starting point for the analysts to choose an initial country/item when there is no clear target in mind (knowing which particular country and food item to look at). Once the analysts pick a country/item pair, they can click on the corresponding cell to further investigate. Here we note that correlation is not equal to causation, so the method of identifying all correlations may suffer from p-fishing. As such, a human in the loop is critical for identifying potential correlations of interest and removing obviously spurious correlations.

4.2 Anomaly Time Series

While correlations are critical for hypothesis generation, our analysts also wanted to be cued to anomalous changes in the trade network or stability time series. By finding anomalies, domain experts can begin reasoning about what other world events may have been contributing to these changes. To support such analyses, we implemented an anomaly time series for the selected country and visualized detected anomalies.

We define an anomaly as any sudden rise or drop from the previous year, which means there could be a shock in the agriculture trade network. To detect anomalies, we first detrend the time series by taking the first difference: $\tilde{y}_t = y_t - y_{t-1}$ for $t \in [2,T]$. Then we compute the mean μ and standard deviation σ of $\{\tilde{y}_t | t \in [2,T]\}$ and define the upper and lower limit as $UL = \mu + 2\sigma$, $LL = \mu - 2\sigma$. Thus, for any time t, a sudden rise ($\tilde{y}_t > UL$) or drop ($\tilde{y}_t < LL$) are detected as an anomaly. Other methods, (e.g. ARIMA [51], EWMA [37]) could also be applied.

For a selected country/item pair, the anomaly time series (Fig. 1 (1)) displays its trade measures, counts of different triads, and social stability (ACLED count and stability) by year. Which type to display can be toggled using the left-side buttons. In addition, the triad counts can be filtered based on the magnitude of the trade relationships using a slider in the top of the interface. This filter is applied to all the triad counts in the networks under analysis throughout the entire framework. For all time series, anomaly detection has been conducted and detected anomalies will be plotted as dots on the corresponding lines. Each anomaly dot can be clicked to investigate countries sharing the same type of anomaly (which occurs in the same year of the same attribute time series). These countries will be displayed as small multiples.

Since there can be multiple time series in the line chart, the analysts can click on the legend to highlight or de-highlight a time series. Whenever the time series is highlighted, a temporal correlation indicator will be displayed to show the correlation between the trade time series and the stability time series from lag 5 to lead 5. The correlations are colored using a diverging color scheme in which the blues encode positive correlations and reds encodes negative correlations. These correlation bars are also shown under each small multiple map to indicate the corresponding correlations for that country.

4.3 Choropleth View

For a selected country and product, we have a main map and a set of small multiples to visualize trade network elements.

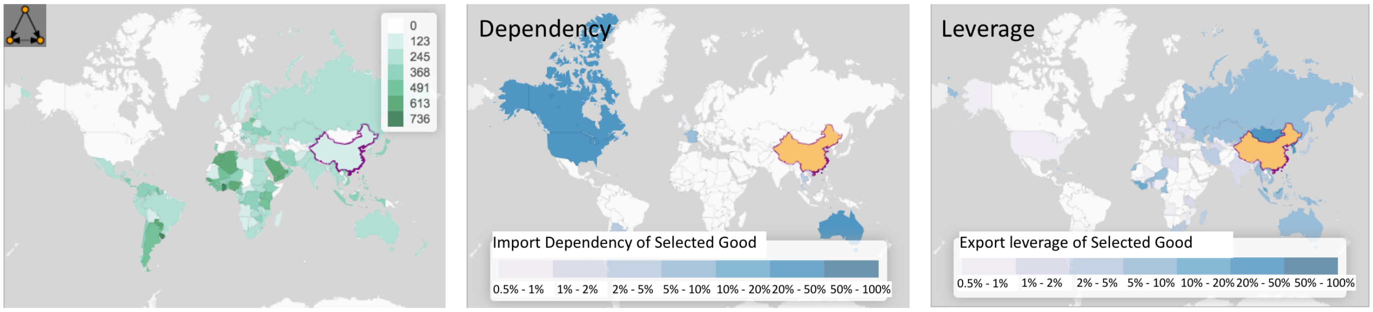

Fig. 4. The main choropleth map can be used to visualize triad, trade quantity/value, and country dependency/leverage. Examples show the triad distribution (left), China's dependency (middle), and China's leverage (right) in cereal network.

The Main Choropleth Map. The main map (Fig. 4) interactively displays the global relationship of other countries to the selected one. It can be switched between trade measures, dependency and leverage, and triad distributions. Users are also allowed to quickly change the selected country by clicking on a country on the map. This choropleth map also supports a detailed overview of a country's core trade products. When mousing over a country, the top 5 import/export products for the country are shown as a bar chart. The value in each bar represents the ratio of the goods' import/export value (or quantity) over the country's total import/export value (or quantity).

Trade Connections and Magnitude. On the main map, the selected country is highlighted in orange and all other countries on the map are colored using a sequential color scale based on the selected measure (trade quantity/value or triad). **Triads** are visualized by the sum of the triad counts in the selected types (out of the 13 types) associated with each country in the food network. **Trade Quantity** is given in tons. When this option is chosen, countries that are in the selected country's trade network are colored based on the imports/exports quantity from/to the selected country. A logarithmic scale is used for better color separation. **Trade Value** is given in dollars. Again, when this option is chosen, countries that are first order members of the selected country's trade network (which means they are directly trading with each other) are colored based on the dollar value of imports/exports from/to the selected country. This color also employs a log scale.

Trade Dependency and Trade Leverage. **Trade dependency** is derived from trade quantity and trade value. The map can show the trade dependency of the selected country to the other countries. The dependency, as explained in Sec. 3.4, has a range of [0, 1]. The color of each country represents how dependent the selected country is to the country. The dependency can be toggled between import and export. The color scale is manually defined to be [0.005, 0.01, 0.02, 0.05, 0.1, 0.2, 0.5, 1] which is approximately logarithmic. **Trade Leverage** is also derived from trade quantity and trade value. The map shows the trade leverage of the selected country to the other countries as described in Sec. 3.4. The colors are defined in the same way as the dependency.

Small Multiple Maps. To help the analyst find similar countries in terms of anomalies, our framework has a small multiple maps view (Fig. 1 (3)) alongside the main map such that for a selected anomaly, the small multiple maps view will display all other countries that have an anomaly in the same year with the same attribute. These small multiples also use choropleth maps to visualize the trade measure centered on these similar countries. The visual setting is synced with the main map. Each of these small multiples was coupled with a colored correlation bar to indicate the temporal correlation of the selected trade attribute to the stability measure. These correlation bars have the same visual encodings as the one in the anomaly time series. Clicking on the label of any small multiple maps will switch the centered country between the main map and the small multiple map, and the other components of the system will update according to the new country selection.

4.4 Trade Diffusion Graph

The trade diffusion graph (Fig. 1 (5)) is used to display the potential impact of an anomaly in the trade network. When there is a sharp decrease or increase in trade for a particular food product, it is tempting to think how such change could be caused by or be causing the trade disruptions of other countries. For example, when there is a sharp decrease in wheat export from China in 2004, many countries experienced a sharp decrease in wheat import in the same year, analysts are interested in knowing whether these countries are directly or indirectly affected by the export drop of China. To explore such questions, we developed the trade diffusion graph, which displays a directed acyclic graph (DAG) connecting the influencing countries to the influenced countries in the same year. Building this graph requires two steps.

Step 1: Identifying source/target countries. Once an anomaly is selected, the list of corresponding trade diffusion source/target countries is queried according to the following rules:

- If the selected anomaly is a sharp decrease (or increase) in exports, we identify target countries with a sharp decrease (or increase) in imports in the same year.
- If the selected anomaly is a sharp decrease (or increase) in imports, we identify source countries with a sharp decrease (or increase) in exports in the same year.

The countries with sharp changes in exports are considered to be the sources of the trade diffusion, while the countries with sharp changes in imports are considered to be the targets. The identified graph will have only one source/target (the selected country) but multiple targets/sources (the identified countries).

Step 2: Identifying diffusion paths. A diffusion path, in our scenario, is defined as a trade path from the source to the target with all links (export to import) that have a higher dependency than a user-defined threshold. To determine if there is such a link from country A to country B: country A may influence country B when $I_{A \to B} > \varepsilon$, where $\varepsilon \in [0,1]$ is a user-defined threshold. We used depth-first search to retrieve these paths, and prune to only keep the paths from the source(s) to the target(s). When the selected country is a source, we would obtain a DAG starting from the selection, and when the selected country is a target, we would obtain a DAG ending to the selection. The graph is drawn using Dagre Javascript library and Jünger and Mutzel's crossing minimization method [38], and the layout of the graph positions the countries based on their topological orders to emphasize the flow of influences from the source country(s)(left) to the target country(s)(right). We encode the strength of dependencies using the width of edges, and each node is labeled by the flag of the corresponding country. Mousing over each country will highlight all the paths between this country and the selected country. The selected country is colored in orange and the other anomalous countries are colored in green. We also provide a slider for interactive adjustment of the dependency threshold.

4.5 Clustering and Comparison

Our analysts wanted the ability to quickly explore similarities across trade and triad profiles and cluster countries based on these attributes. They would like to see if similar countries might have the same vulnerability in the trade network or may be impacted by the same change happened in the network that could cause some social instability.

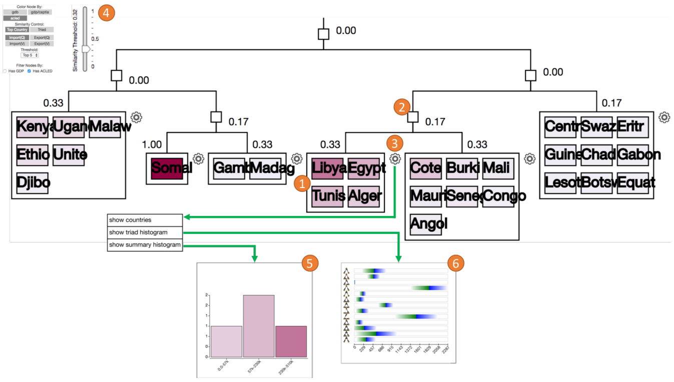

Fig. 5. The Clustering View displays the clusters of countries in a dendrogram. Countries in a cluster are grouped in a box (1). Clicking on any box will break the cluster into two smaller clusters. Clicking on any internal node (2) collapses all children. The analyst can use the slider (4) to adjust the similarity threshold for the hierarchical clustering. The color of the countries encodes their selected stability measure. By clicking on the setting icon (3) at the top right corner of each box, the analyst can choose between different view options for the box. The box can change to a histogram of the stability measure (5) or a bar chart that compares the mean and the standard deviation of every triad configuration (6).

Scatter Plot. To enable further comparison and correlation analysis, we have created a scatter plot view (Fig. 7 (3)) which displays the countries' network attributes versus ACLED counts, GDP, or GDP per capita. The analysts can use the selected boxes next to each of the axes to toggle either the attributes or scales (linear, square root, and log).

Clustering Visualization. We have integrated a hierarchical clustering view for interactive clustering analysis. The countries are clustered using a complete-link hierarchical clustering algorithm. If we cut the hierarchy using a similarity threshold, the nodes whose minimum similarities are at least equal to the similarity threshold can form clusters. We display the clusters in a dendrogram (Fig.5). In this view, the clusters are represented by a box enclosing a set of rectangles, where each rectangle represents a country. The internal nodes of the hierarchy are drawn above the boxes with a similarity threshold at which the descendants will merge. The number next to each box represents the minimum similarity of countries within the box, and the number next to each internal node represents the minimum similarity of all countries under this node. Initially, the clusters are formed according to a default threshold, 0.5. The analyst can drag the slider to change the similarity threshold or click on a box or an internal node to expand or collapse the cluster. Clicking on any box will expand the hierarchy by splitting the countries in this box into two clusters and make the current box an internal node connecting these two clusters. Clicking on an internal node will collapse the hierarchy by joining all the boxes below the node into a larger box , and the internal node will be replaced by the newly created box. The color in each of the internal rectangles encodes the value of either the GDP, the GDP per capita, or the number of violent events in the country which the rectangle represents.

Clustering utilizes partner similarity or triad similarity.

Triad Similarity. This metric defines the country similarity by comparing their triad profiles. A country's triad profile is defined as a vector of the frequencies that the country appears in each triad configuration. Thus, when using positional triad configurations, the country's triad profile is a 13×1 vector where each entry represents one frequency. The triad similarity of two countries is then defined as the vector similarity of their triad profiles. We used Euclidean distance to calculate this similarity. By default, all entries in the triad profile are used for the similarity calculation. The analyst can filter out some types of the triad configurations using the control panel (under the similarity control area) so that the similarity is calculated only on the selected entries.

Trade Partner Similarity. This metric defines the country similarity by comparing its most important trading partners in the network. Given country c_i and c_j, we can define the set of their trade partners as T_{c_i} and T_{c_j}, and then the partner similarity between these two countries can be defined as $|T_{c_i} \cap T_{c_j}|$. Interactive filters can be employed such that T_{c_i} can represent only the N largest trade partners. In this way, we can look for countries whose largest trade partners share a large set overlap.

Cluster Exploration. Detailed exploration of the grouped country in a box is available in our framework. In the top-right corner of each, a configuration icon is found. The analyst can click on the configuration icon to switch between three visualization options for displaying the country cluster. The default is to list the countries, as displayed on the top of Figure 5. The second option switches this view to a histogram, as shown on the lower left of Figure 5. It can be either the triad summary histogram or the data summary histogram. In the data summary histogram, the violence count, GDP or GDP per-capita of all countries within the cluster are summarized. In the triad summary histogram, as shown in the lower right of Figure 5, each bar shows the mean of the count of one type of triad configuration for all countries in the cluster. The length of the green color area represents one standard deviation below the mean, and the blue color area represents one standard deviation above the mean.

5 Case Studies

Our case studies were developed by our domain experts in political science and sustainability. Training and paired analysis was used initially, and then experts took our tool and integrated it into their current data analysis process. In this section, we provide details on their findings and hypotheses generated when using our visual analytics framework.

5.1 2011 East Asia Drought and Flood

Thailand is a major rice exporter globally and is typically subject to severe flooding. However, Thailand has recently suffered several years of extreme drought beginning in 2011 [26]. Our analysts were interested in performing an exploratory analysis focused on the global impacts of localized climate events. In our first case study, we demonstrate how this tool was used to develop hypotheses about how changes in Thailand's rice exports might induce potential social unrest in Africa.

First, the analyst selected rice and Thailand. The line chart showed a significant decrease in the quantity of rice exports in 2012 (Fig. 1(1)). While this was not surprising given Thailand's agriculture disruption in 2011, it did establish that the drought was followed by a drop in exports the following year. To see which countries might be significantly impacted due to this export drop, the analyst clicked on the anomaly dot on Thailand's export line. Small multiple maps listed all countries which also had significant drops in rice exports in 2012. On the trade diffusion graph (Fig. 1(5)), countries that experienced a decrease in rice imports were retrieved and linked by their dependencies to Thailand. The resulting graph showed that some countries, such as Niger, United States, India, China, and Vietnam, transferred this impact to other trade partners but were not significantly impacted by Thailand's rice export shrinkage, while many other countries, marked with the green background, suffered large decreases in import quantities of rice.

The analyst then wanted to explore why some countries suffered from Thailand's rice export decrease more significantly than others. In particular, he wished to know if this might be related to their trade network structures. He clustered these countries shown on the trade diffusion graph using triad similarity. The clustering result, with a threshold of 0.5, is shown in Fig. 1(4). A finding of interest to the analyst is that the largest group (Tunisia, Niger, etc.) contains most of the countries that were affected by Thailand's drop in rice exports. When the analyst split the largest grouping, he noticed that the remaining countries in the group were all the countries that experienced the rice anomaly, except Fiji. By switching to view the average triad profile in each cluster, the analyst noticed most of the variability among these clusters came from the open triads (type 1 to 6 on Fig. 2). Thus, the analyst then chose to remove the closed triads in the clustering control panel and re-cluster the countries. He found that the countries with import anomalies were more tightly grouped together. Looking at the trade diffusion graph again, the analyst quickly noticed that countries that were initially out of the largest cluster had leverages on multiple countries. For example, Pakistan, though marked with the green

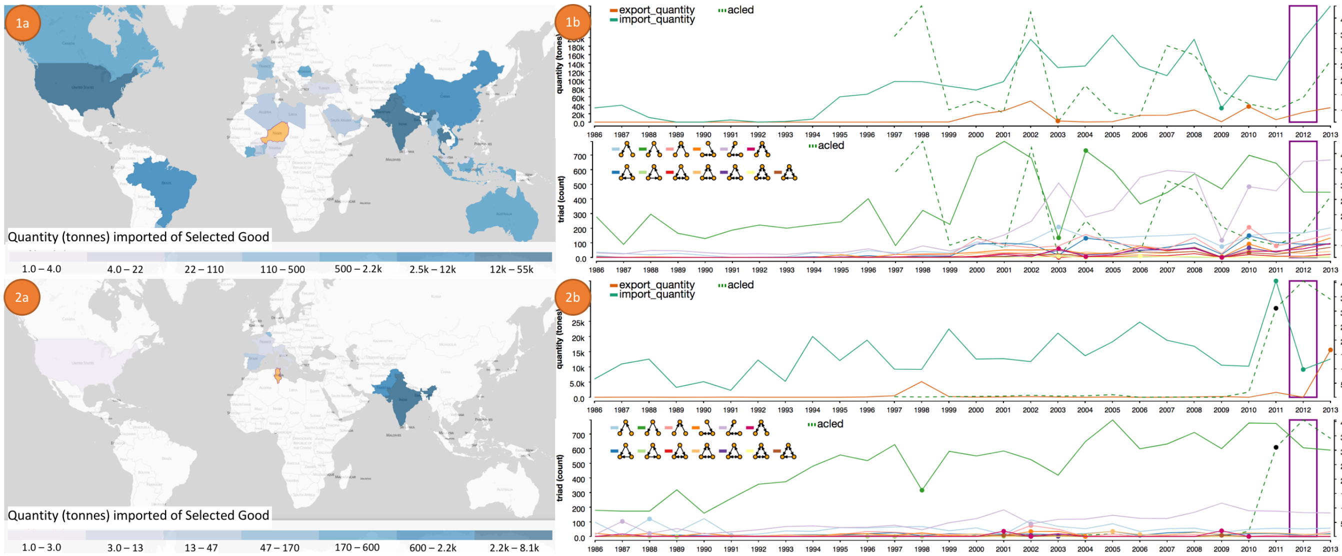

Fig. 6. Comparison between Niger (1) and Tunisia (2) on each country's import quantity of rice. By comparing both countries' major exporters of rice using the choropleth views (1a, 2a), it can be seen that Niger imports from a wide variety of countries whereas Tunisia imports primarily from India and Pakistan. The time series for both countries (1b, 2b) show that Tunisia had an import quantity dip in 2012 while Niger had no such disruption. At the same time, Tunisia had a sharp increase in local conflict events. The analyst can also observe that Tunisia had fewer types of triads than Niger.

background, also served as a transferring country in the network as it had multiple leverages on Iran, Kuwait, and Tunisia, and it had a large amount of the Fig. 2 type (2) open triad. All the other anomalous countries had no leverages on other countries, and Fiji, along with most other countries that were later separated from the largest group (Australia, Cambodia, and Niger) only leveraged on one country in this graph, and this group of countries had significantly less type (2) triads. These findings indicate that by using triad profiles, it may be possible to group countries based on their leverage on other countries. Our analyst noted that this can be a testable hypothesis for future research.

Recalling that our analyst was interested in finding possible relationships between a country's trade network and its social stability, he decided to further explore Tunisia and Niger which, in general, have local conflict problems. He sought to understand why Tunisia had an anomaly while Niger did not, and whether this anomaly could be relevant to their local unrest events. The analyst clicked on these two countries to check their import quantity and ACLED event line charts. As shown in Fig. 6, Tunisia had an import quantity dip in 2012 while Niger had no such disruption. At the same time, Tunisia had a dramatically increased number of local conflict events, and the ACLED line shows a sharp rise during 2011 and 2012. Although the exact relationship between rice imports and local armed conflicts cannot conclusively be determined here, it nevertheless provides evidence that these two variables may be related, as their anomalies happened close in time.

To see how this is related to Niger's and Tunisia's rice trade, the analyst inspected their worldwide import quantities. As shown in Fig. 6, Tunisia imports most of its rice from India and Pakistan, both of which are in the trade diffusion graph of Thailand's export cut. However, Niger imports rice from a wide number of countries, including Brazil, Canada, and Australia, which are not all in the diffusion graph and not shown in the small multiple maps (meaning they did not have significant drops in rice exports). As such, having a wide trade network that does not connect in a single trade diffusion path can increase a country's resilience to agriculture disruption. It may also enhance local stability, as Niger did not exhibit a significant social unrest problem like those in Tunisia. Regarding triads, the analyst compared these two countries on the scatter plot and their triad line charts. As expected, Tunisia had fewer types of triads than Niger.

5.2 Sustainability - Food Insecurity and Political Instability

Our second case study was provided by a domain expert in sustainability who focused on using the framework from the perspective of stakeholders in the international development and aid community. In particular, he used the framework to suggest geographical regions where decision makers in his domain may want to focus their attention. In this case, the analyst sought to identify potential hotspots of political instability arising from food insecurity.

Our analyst started by examining the country-product matrix and focused on cereal (a proxy for wheat in this dataset). The matrix indicated that, for both Mauritania and Cameroon, several correlations were detected between their cereal trade measures and social unrest events (Fig. 3). Knowing that Mauritania's main agricultural products are wheat, grain, and corn (part of the cereal category), while Cameroon's are coffee, sugar, and tobacco, but not cereal, the analyst expected that Cameroon would rely more on imports of cereal than did Mauritania. To confirm this, he looked at the line charts for cereal import values and quantities of both countries and found that, on average, Cameroon's import of cereal was twice that of Mauritania. Furthermore, the analyst found that, for Cameroon, during 2011 and 2012, the import value of cereal increased significantly, though the quantity only slightly increased. This indicated a probable price increase in cereal, which matched the global wheat price hikes in early August 2011 as wheat production and markets were disrupted by natural disasters (e.g., 2010 Russian wheat crops were lost in wildfires and led to decreases its 2010/2011 production and stock). Turning specifically to wheat (a subcategory under cereal), the analyst found that Egypt (a similar country pulled from the small multiple maps) experienced a significant price increase for imported wheat. The line chart revealed that not only did Egypt's import value of cereal products exhibit high positive correlation with ACLED events, but Egypt also had an uncharacteristic increase in cereal imports in 2011 followed by an anomalous increase in ACLED events in 2013. This could suggest that the surge of ACLED events were caused partly by rising food prices.

Next, our domain expert chose to explore what other countries also experienced a sudden increase in cereal imports in 2011. He did this by clicking the anomaly indicator on the import value time series, which loaded a list of countries on the small multiple map view. The domain expert immediately noticed Algeria on the list, whose import value also had a high positive correlation with ACLED events (shown by the mini correlation bar underneath the map). Scrolling down the list, the analyst also noted Lebanon and Yemen, both of which experienced uprisings during this time. The analyst moved these countries to the top of the list by clicking on the checkbox on the top left corner of their maps and compared their cereal exporters. He noticed that all

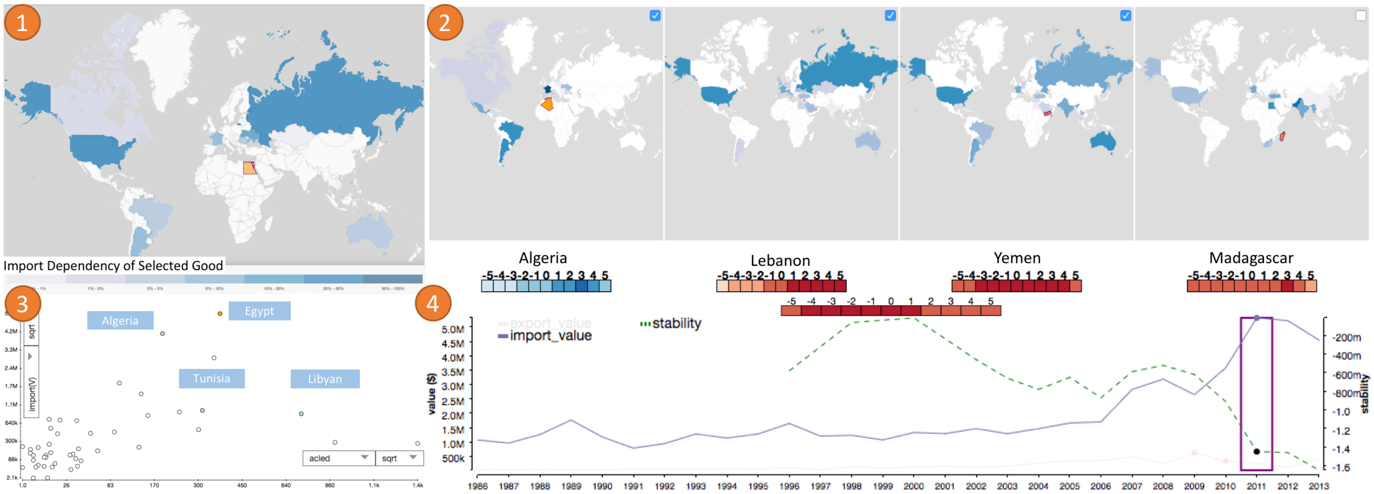

Fig. 7. Egypt had a sharp increase in cereal import value in 2011. This figure shows (1) the import value distribution of Egypt, (2) the similar countries who had the same increase, (3) the scatter plot by ACLED and import value of cereal among Africa countries, and (4) the time series indicating the sharp increase as well as the negative correlation between Egypt's import value and its stability index.

four countries imported wheat from a majority of the same exporters, with the exception that Algeria was less reliant on Russia. The domain expert then switched the target of correlation comparison to the stability index and found that Egypt, Yemen, and Lebanon all had a strong negative correlation with the stability index, while Algeria did not. These findings suggest that the sudden increase in the import value negatively correlates with stability for Egypt, Lebanon, and Yemen and that this negative correlation might be due to the similarity of their import patterns. In addition, their triad profiles have a similar distribution and all show that triad type (5) and (1) are the most common.

Finally, our domain expert chose to explore which other countries had cereal trade structures similar to that of Egypt. His presumption was that if such countries substantially share the same global structure for wheat trade, they may be at risk for episodes of political instability similar to those witnessed in Egypt. Therefore, the analyst performed a clustering on trade partner similarity and found that Egypt, Libya, Tunisia, and Algeria were clustered together (Fig. 5).

In assessing the veracity of these suggested focal countries, our analyst noted that in 2011, civil war erupted in both Syria and Libya, with Lebanon becoming engulfed in the Syrian conflict by 2012. Internal rifts also escalated into civil war in Yemen in 2014, while in 2013 the Council on Foreign Relations reported that the risk of political instability in Jordan had reached its highest level in over 40 years [66]. Additionally, Algeria and Tunisia experienced political unrest to varying degrees during this same time frame. While appearing to support the notion that the tool's trade similarity analysis may accurately focus a user's attention, our domain expert also cautioned that these examples are admittedly anecdotal. Both our experts found that the tool provided unique capabilities for hypothesis generation that were unavailable through their current workflow; however, the ability to couple this with analyses for hypothesis testing was further requested.

6 Conclusion and Future Work

In this paper, we have demonstrated a visual analytics framework for spatiotemporal trade network analysis. Our framework focuses on network feature analysis and enables users to quickly identify temporal anomalies within these features as well as correlate these features to country level stability indicators. By linking multisource data for exploration, our framework enables users to explore and develop complex hypotheses. While several visual analytics systems have explored trade network analysis, our framework focuses specifically on integrating triad analysis with other metrics to provide novel insights.

Our framework has been designed and evaluated through collaboration with domain experts from the Global Security Initiative and the School of Politics and Global Studies at Arizona State University. Examples ranged from exploring theories of Capitalist Peace to food insecurity and instability cascading through the trade network. Our partners found that the anomaly detection provided them with a clever means of identifying regions and time periods of interest, and while they relied on their own domain knowledge as a starting point, they noted that they planned to do further exploration to see what other hypotheses might be developed with a deeper dive into unexplored anomalies. Both the clustering view and the small multiples anomaly view were key features in their analytic process; however, both analysts noted that the framework could only support exploratory data analysis.

Reflecting on the design of the system, there are a variety of challenges that must still be addressed. Given the highly multivariate nature of the data, and the need to identify lags/leads in conjunction with potential network disruptions, numerous anomalies are detected. It is unlikely that the initial analysis step in the visual analytics process will be completely sufficient for discovering unexpected patterns. While our designs attempted to provide an overview of anomalies through a country-product matrix view, new visualization designs should focus on improving the overview, as well as combining a suite of analytic methods that can vote on most likely anomalies. Here, the tradeoff of reducing the number of anomalies for exploration versus missing an event needs to be considered. We also note the limitations of choropleth maps in our design. While these maps directly support analysts with a familiar structure, the sheer number of countries and trade goods that exist in the dataset limits their functionality. Again, these maps provide an overview and serve the analyst well for filtering; however, new views that can highlight multivariate trade over should also be explored. Sankey diagrams may serve as an alternative, or dynamic network visualization techniques (e.g. [6]) may be advantageous.

The current limitation of our work is that it still falls short in identifying spurious correlations. While the current framework can provide many useful clues about the interdependency of trade between countries and the effect of such interdependency on social stabilities, it does not provide a way to justify the findings and exclude other possible explanations. The analyst must rely on external sources to verify the results. For future work, we will explore extensions of the system to support a workflow that also incorporates hypothesis testing. Such an extension will likely require novel interactions and new views to support exploratory analysis and the hypothesis testing.

7 Acknowledgements

This work is supported by the U.S. Department of Homeland Security under Award Number, 2017-ST-061-QA0001 and the National Science Foundation, Grant Nos. 1350573 and 1639227. The views and conclusions contained in this document are those of the authors and should not be interpreted as necessarily representing the official policies, either expressed or implied, of the U.S. Department of Homeland Security.

REFERENCES

[1] Food and agriculture organization of the united nations statistics division. http://www.fao.org/faostat/en/#home, 2015.

[2] N. Adrienko and G. Adrienko. Spatial generalization and aggregation of massive movement data. *IEEE Transactions on Visualization and Computer Graphics*, 17(2):205–219, 2011.

[3] G. Andrienko and N. Andrienko. Spatio-temporal aggregation for visual analysis of movements. In *IEEE Symposium on Visual Analytics Science and Technology*, pp. 51–58. IEEE, 2008.

[4] L. Bargigli, G. di Iasio, L. Infante, F. Lillo, and F. Pierobon. The multiplex structure of interbank networks. *Quantitative Finance*, 15(4):673–691, 2015.

[5] M. Barigozzi, G. Fagiolo, and G. Mangioni. Identifying the community structure of the international-trade multi-network. *Physica A: Statistical Mechanics and its Applications*, 390(11):2051–2066, June 2011.

[6] F. Beck, M. Burch, S. Diehl, and D. Weiskopf. A taxonomy and survey of dynamic graph visualization. In *Computer Graphics Forum*, vol. 36, pp. 133–159. Wiley Online Library, 2017.

[7] I. Boyandin, E. Bertini, P. Bak, and D. Lalanne. Flowstrates: An approach for visual exploration of temporal origin-destination data. In *Computer Graphics Forum*, vol. 30, pp. 971–980. Wiley Online Library, 2011.

[8] I. Boyandin, E. Bertini, and D. Lalanne. Using flow maps to explore migrations over time. In *Geospatial Visual Analytics Workshop in conjunction with The 13th AGILE International Conference on Geographic Information Science*, vol. 2, 2010.

[9] K. Buchin, B. Speckmann, and K. Verbeek. Angle-restricted steiner arborescences for flow map layout. In *International Symposium on Algorithms and Computation*, pp. 250–259. Springer, 2011.

[10] K. Buchin, B. Speckmann, and K. Verbeek. Flow map layout via spiral trees. *IEEE Transactions on Visualization and Computer Graphics*, 17(12):2536–2544, 2011.

[11] D. Cartwright and F. Harary. Structural balance: a generalization of heider's theory. *Psychological Review*, 63(5):277–293, 1956.

[12] J. Chae, Y. Cui, Y. Jang, G. Wang, A. Malik, and D. S. Ebert. Trajectory-based Visual Analytics for Anomalous Human Movement Analysis using Social Media. In E. Bertini and J. C. Roberts, eds., *EuroVis Workshop on Visual Analytics*. The Eurographics Association, 2015.

[13] J. Chae, D. Thom, H. Bosch, J. Yang, R. Maciejewski, D. S. Ebert, and T. Ertl. Spatiotemporal Social Media Analytics for Abnormal Event Detection and Examination using Seasonal-Trend Decomposition. In *IEEE Conference on Visual Analytics Science and Technology*, Oct. 2012.

[14] V. Chandola, A. Banerjee, and V. Kumar. Anomaly detection: A survey. *ACM computing surveys (CSUR)*, 41(3):15, 2009.

[15] K. C. Cox, S. G. Eick, and T. He. 3d geographic network displays. *ACM Sigmod Record*, 25(4):50–54, 1996.

[16] W. Cui, H. Zhou, H. Qu, P. C. Wong, and X. Li. Geometry-based edge clustering for graph visualization. *IEEE Transactions on Visualization and Computer Graphics*, 14(6):1277–1284, 2008.

[17] C. Dalin, M. Konar, N. Hanasaki, A. Rinaldo, and I. Rodriguez-Iturbe. Evolution of the global virtual water trade network. *Proceedings of the National Academy of Sciences*, 109(16):5989–5994, Apr. 2012.

[18] L. De Benedictis and L. Tajoli. Comparing Sectoral International Trade Networks. *Aussenwirtschaft*, (65):167–189, 2010.

[19] L. De Benedictis and L. Tajoli. The world trade network. *The World Economy*, 34(8):1417–1454, 2011.

[20] M. Dodge and R. Kitchin. Charting movement: mapping internet infrastructures. In *Moving People, Goods and Information in the Twenty First Century: Urban Technology, the New Economy, and Cutting-Edge Infrastructure*, pp. 159–185. Spon Press, New York, 2003.

[21] W. Dou, X. Wang, D. Skau, W. Ribarsky, and M. X. Zhou. Leadline: Interactive visual analysis of text data through event identification and exploration. In *IEEE Conference on Visual Analytics Science and Technology*, pp. 93–102. IEEE, 2012.

[22] G. Facchetti, G. Iacono, and C. Altafini. Computing global structural balance in large-scale signed social networks. *Proceedings of the National Academy of Sciences*, 108(52):20953–20958, 2011.

[23] G. Fagiolo and M. Mastrorillo. Does human migration affect international trade? a complex-network perspective. *PloS one*, 9(5):e97331, 2014.

[24] G. Fagiolo, J. Reyes, and S. Schiavo. The evolution of the world trade web: a weighted-network analysis. *Journal of Evolutionary Economics*, 20(4):479–514, Aug. 2010.

[25] K. Faust. Very local structure in social networks. *Sociological Methodology*, 37:209–256, 2007.

[26] F. Franzetti, A. Pezzoli, and M. Baliani. *Rethinking Water Resources Management Under a Climate Change Perspective: From National to Local Level. The Case of Thailand*, pp. 169–195. Springer, Cham, Switzerland, 2017.

[27] D. Garlaschelli and M. I. Loffredo. Fitness-Dependent Topological Properties of the World Trade Web. *Physical Review Letters*, 93(18):188701, Oct. 2004.

[28] D. Garlaschelli and M. I. Loffredo. Structure and evolution of the world trade network. *Physica A: Statistical Mechanics and its Applications*, 355(1):138–144, Sept. 2005.

[29] D. Garlaschelli, T. D. Matteo, T. Aste, G. Caldarelli, and M. I. Loffredo. Interplay between topology and dynamics in the World Trade Web. *The European Physical Journal B*, 57(2):159–164, May 2007.

[30] D. Gotz and H. Stavropoulos. Decisionflow: Visual analytics for high-dimensional temporal event sequence data. *IEEE Transactions on Visualization and Computer Graphics*, 20(12):1783–1792, 2014.

[31] D. Guo. Flow Mapping and Multivariate Visualization of Large Spatial Interaction Data. *IEEE Transactions on Visualization and Computer Graphics*, 15(6):1041–1048, Nov. 2009.

[32] D. Guo and X. Zhu. Origin-Destination Flow Data Smoothing and Mapping. *IEEE Transactions on Visualization and Computer Graphics*, 20(12):2043–2052, 2014.

[33] R. A. Hanneman and M. Riddle. *Introduction to social network methods*. University of Riverside, Riverside, California, USA, 2005.

[34] P. W. Holland and S. Leinhardt. Local structure in social networks. *Sociological Methodology*, 7:1–45, 1976.

[35] D. Holten and J. J. Van Wijk. Force-directed edge bundling for graph visualization. In *Computer graphics forum*, vol. 28, pp. 983–990. Wiley Online Library, 2009.

[36] S. M. Hsiang, K. C. Meng, and M. A. Cane. Civil conflicts are associated with the global climate. *Nature*, 476(7361):438–441, 2011.

[37] J. S. Hunter. The exponentially weighted moving average. *Journal of quality technology*, 18(4):203–210, 1986.

[38] M. Jünger and P. Mutzel. 2-layer straightline crossing minimization: Performance of exact and heuristic algorithms. In *Graph Algorithms And Applications I*, pp. 3–27. World Scientific, 2002.

[39] P. Kaluza, A. Kölzsch, M. T. Gastner, and B. Blasius. The complex network of global cargo ship movements. *Journal of The Royal Society Interface*, 2010.

[40] P. Kaluza, A. Klzsch, M. T. Gastner, and B. Blasius. The complex network of global cargo ship movements. *Journal of The Royal Society Interface*, Jan. 2010.

[41] K. Kanemoto, D. Moran, M. Lenzen, and A. Geschke. International trade undermines national emission reduction targets: New evidence from air pollution. *Global Environmental Change*, 24:52–59, 2014.

[42] D. Kaufmann, A. Kraay, and M. Mastruzzi. The worldwide governance indicators: methodology and analytical issues. *Hague Journal on the Rule of Law*, 3(2):220–246, 2011.

[43] D. A. Keim, F. Mansmann, and J. Thomas. Visual Analytics: How Much Visualization and How Much Analytics? *SIGKDD Explor. Newsl.*, 11(2):5–8, May 2010.

[44] M. Konar, C. Dalin, S. Suweis, N. Hanasaki, A. Rinaldo, and I. Rodriguez-Iturbe. Water for food: The global virtual water trade network. *Water Resources Research*, 47(5):W05520:1–17, May 2011.

[45] S. C. Lee, R. G. Muncaster, and D. A. Zinnes. The friend of my enemy is my enemy: Modeling triadic internation relationships. *Synthese*, 100(3):333–358, 1994.

[46] Y. Lu, M. Steptoe, S. Burke, H. Wang, J.-Y. Tsai, H. Davulcu, D. Montgomery, S. R. Corman, and R. Maciejewski. Exploring evolving media discourse through event cueing. *IEEE Transactions on Visualization and Computer Graphics*, 22(1):220–229, 2016.

[47] Y. Lu, H. Wang, S. Landis, and R. Maciejewski. A visual analytics framework for identifying topic drivers in media events. *IEEE Transactions on Visualization and Computer Graphics*, PP(99):1–1, 2018.

[48] W. Luo, P. Yin, Q. Di, F. Hardisty, and A. M. MacEachren. A geovisual analytic approach to understanding geo-social relationships in the international trade network. *PloS one*, 9(2):e88666, 2014.

[49] G. K. MacDonald, K. A. Brauman, S. Sun, K. M. Carlson, E. S. Cassidy, J. S. Gerber, and P. C. West. Rethinking agricultural trade relationships in an era of globalization. *BioScience*, p. biu225, 2015.

[50] E. Mäkinen and H. Siirtola. Reordering the reorderable matrix as an algorithmic problem. In *International Conference on Theory and Application*

of Diagrams, pp. 453–468. Springer, 2000.

[51] S. Makridakis and M. Hibon. Arma models and the box–jenkins methodology. *Journal of Forecasting*, 16(3):147–163, 1997.

[52] A. Malik, R. Maciejewski, N. Elmqvist, Y. Jang, D. S. Ebert, and W. Huang. A correlative analysis process in a visual analytics environment. In *IEEE Conference on Visual Analytics Science and Technology*, pp. 33–42. IEEE, 2012.

[53] M. G. Marshall. Fragility, instability, and the failure of states. *Center for*, 2008.

[54] J. J. McCarthy. *Climate change 2001: impacts, adaptation, and vulnerability: contribution of Working Group II to the third assessment report of the Intergovernmental Panel on Climate Change*. Cambridge University Press, 2001.

[55] R. Milo, S. Itzkovitz, N. Kashtan, R. Levitt, S. Shen-Orr, I. Ayzenshtat, M. Sheffer, and U. Alon. Superfamilies of evolved and designed networks. *Science*, 303(5663):1538–1542, 2004.

[56] R. Milo, S. Shen-Orr, S. Itzkovitz, N. Kashtan, D. Chklovskii, and U. Alon. Network motifs: simple building blocks of complex networks. *Science*, 298(5594):824–827, 2002.

[57] Z. Moaz. *Networks of nations: The evolution, structure, and impact of international networks, 1816-2001*, vol. 32 of *Structural analysis in the social sciences*. Cambridge University Press, New York, 2011.

[58] T. Munzner, E. Hoffman, K. Claffy, and B. Fenner. Visualizing the global topology of the mbone. In *Proceedings IEEE Symposium on Information Visualization*, pp. 85–92. IEEE, 1996.

[59] A. Nocaj and U. Brandes. Stub bundling and confluent spirals for geographic networks. In *International Symposium on Graph Drawing*, pp. 388–399. Springer, 2013.

[60] D. Phan, L. Xiao, R. Yeh, and P. Hanrahan. Flow map layout. In *IEEE Symposium on Information Visualization, 2005*, pp. 219–224. IEEE, 2005.

[61] C. Prell and J. Skvoretz. Looking at social capital through triad structures. *Connections*, 28(2):4–16, 2008.

[62] A. Rae. From spatial interaction data to spatial interaction information? geovisualisation and spatial structures of migration from the 2001 uk census. *Computers, Environment and Urban Systems*, 33(3):161–178, 2009.

[63] C. Raleigh, A. Linke, H. Hegre, and J. Karlsen. Introducing ACLED: An armed conflict location and event dataset. *Journal of Peace Research*, 47(5):651–660, 2010.

[64] J. Reyes, S. Schiavo, and G. Fagiolo. Using complex network analysis to assess the evolution of international economic integration: The cases of East Asia and Latin America. Technical Report 2007/25, LEM Working Paper Series, 2007.

[65] J. A. Reyes and R. Kali. The Architecture of Globalization: A Network Approach to International Economic Integration. Technical Report ID 922059, Social Science Research Network, Rochester, NY, May 2006.

[66] R. Satloff and D. Schenker. Contingency planning memorandum no. 19: Political instability in jordan. Technical report, Council on Foreign Relations, Washginton, DC, May 2013.

[67] R. Scheepens, H. van de Wetering, and J. J. van Wijk. Contour based visualization of vessel movement predictions. *International Journal of Geographical Information Science*, 28(5):891–909, 2014.

[68] R. Scheepens, N. Willems, H. van de Wetering, and J. van Wijk. Interactive Density Maps for Moving Objects. *IEEE Computer Graphics and Applications*, 32(1):56–66, 2012.

[69] P. Shi, J. Zhang, B. Yang, and J. Luo. Hierarchicality of trade flow networks reveals complexity of products. *PloS one*, 9(6):e98247, 2014.

[70] S. T. Shutters and R. Muneepeerakul. Agricultural Trade Networks and Patterns of Economic Development. *PLOS ONE*, 7(7):e39756:1–9, July 2012.

[71] D. B. Stouffer, M. Sales-Pardo, M. I. Sirer, and J. Bascompte. Evolutionary conservation of species' roles in food webs. *Science*, 335(6075):1489–1492, 2012.

[72] S. Suweis, M. Konar, C. Dalin, N. Hanasaki, A. Rinaldo, and I. Rodriguez-Iturbe. Structure and controls of the global virtual water trade network. *Geophysical Research Letters*, 38(10):L10403, May 2011.

[73] M. Szell and S. Thurner. Measuring social dynamics in a massive multiplayer online game. *Social Networks*, 32(4):313–329, 2010.

[74] D. Thom, H. Bosch, S. Koch, M. Wörner, and T. Ertl. Spatiotemporal anomaly detection through visual analysis of geolocated twitter messages. In *Pacific visualization symposium*, pp. 41–48. IEEE, 2012.

[75] W. R. Tobler. Experiments in migration mapping by computer. *The American Cartographer*, 14(2):155–163, 1987.

[76] United States Department of Defense. Quadrennial Defense Review Report, 2014.

[77] S. Wasserman and K. Faust. *Social Network Analysis: Methods and Applications*. Structural Analysis in the Social Sciences. Cambridge University Press, New York, 1994.

[78] J. S. Waters and J. H. Fewell. Information processing in social insect networks. *PLoS One*, 7(7):e40337, 2012.

[79] J. Wood, J. Dykes, and A. Slingsby. Visualisation of Origins, Destinations and Flows with OD Maps. *The Cartographic Journal*, 47(2):117–129, May 2010.

[80] Y. Yang, T. Dwyer, S. Goodwin, and K. Marriott. Many-to-many geographically-embedded flow visualisation: An evaluation. *IEEE Transactions on Visualization and Computer Graphics*, 23(1):411–420, 2017.

[81] J. Yoon, S. R. Thye, and E. J. Lawler. Exchange and cohesion in dyads and triads: A test of simmels hypothesis. *Social science research*, 42(6):1457–1466, 2013.

[82] L. Zhang, G. Qian, and L. Zhang. Network motif & triad significance profile analyses on software system. *W. Trans. on Comp.*, 7(6):756–765, 2008.